HHS Public Access

Author manuscript

Neuroimage. Author manuscript; available in PMC 2017 January 01.

Published in final edited form as:

Neuroimage. 2016 January 1; 124(Pt A): 714–723. doi:10.1016/j.neuroimage.2015.09.030.

Combining task-evoked and spontaneous activity to improve pre-operative brain mapping with fMRI

Michael D. Fox[*,1,2,3], **Tianyi Qian**[*,2,4], **Joseph R. Madsen**[5], **Danhong Wang**[2], **Meiling Li**[2], **Manling Ge**[6], **Huan-cong Zuo**[7], **David M. Groppe**[8,9,10], **Ashesh D. Mehta**[8,9], **Bo Hong**[4], and **Hesheng Liu**[2]

[1]Berenson-Allen Center for Noninvasive Brain Stimulation, Department of Neurology, Beth Israel Deaconess Medical Center and Harvard Medical School, Boston, MA, USA

[2]Athinoula A. Martinos Center for Biomedical Imaging, Massachusetts General Hospital, Harvard Medical School, Boston, MA, USA

[3]Department of Neurology, Massachusetts General Hospital, Harvard Medical School, Boston, MA, USA

[4]Department of Biomedical Engineering, School of Medicine, Tsinghua University, Beijing, China

[5]Department of Neurosurgery, Boston Children's Hospital, Harvard Medical School, Boston, MA, USA

[6]Key Laboratory of Electromagnetic Field and Electrical Apparatus Reliability, Department of Biomedical Engineering, Hebei University of Technology, Tianjin, China

[7]Second Affiliated Hospital of Tsinghua University, Beijing, China

[8]Department of Neurosurgery, Hofstra North Shore LIJ School of Medicine, 300 Community Dr., Manhasset, NY 11030

[9]Feinstein Institute for Medical Research, 350 Community Dr., Manhasset, NY 11030, USA

[10]Department of Psychology, University of Toronto, 100 St. George St., Toronto, ON M5S 3G3, Canada

Abstract

Noninvasive localization of brain function is used to understand and treat neurological disease, exemplified by pre-operative fMRI mapping prior to neurosurgical intervention. The principal approach for generating these maps relies on brain responses evoked by a task and, despite known limitations, has dominated clinical practice for over 20 years. Recently, pre-operative fMRI mapping based on correlations in spontaneous brain activity has been demonstrated, however this

Address Correspondence To: Dr. Hesheng Liu, Suite 2301, 149 13th St., Athinoula A. Martinos Center for Biomedical Imaging, Massachusetts General Hospital, Charlestown, MA, 02129, Hesheng@nmr.mgh.harvard.edu Or Dr. Bo Hong, Department of Biomedical Engineering, School of Medicine, Tsinghua University, Beijing, 100084, China, Hongbo@tsinghua.edu.cn.

*These authors contributed equally to this work

approach has its own limitations and has not seen widespread clinical use. Here we show that spontaneous and task-based mapping can be performed together using the same pre-operative fMRI data, provide complimentary information relevant for functional localization, and can be combined to improve identification of eloquent motor cortex. Accuracy, sensitivity, and specificity of our approach are quantified through comparison with electrical cortical stimulation mapping in eight patients with intractable epilepsy. Broad applicability and reproducibility of our approach is demonstrated through prospective replication in an independent dataset of six patients from a different center. In both cohorts and every individual patient, we see a significant improvement in signal to noise and mapping accuracy independent of threshold, quantified using receiver operating characteristic curves. Collectively, our results suggest that modifying the processing of fMRI data to incorporate both task-based and spontaneous activity significantly improves functional localization in pre-operative patients. Because this method requires no additional scan time or modification to conventional pre-operative data acquisition protocols it could have widespread utility.

INTRODUCTION

The most common clinical application of functional magnetic resonance imaging (fMRI) is pre-operative brain mapping to help guide neurosurgical intervention (Dimou et al., 2013; Matthews et al., 2006; Vlieger et al., 2004). The traditional pre-operative mapping approach uses intermittent periods of task to activate and identify brain areas to be avoided during surgery, such as finger tapping to identify primary motor cortex. First used for pre-operative mapping over 20 years ago (Desmond et al., 1995; Jack et al., 1994), this task-based strategy continues to dominate clinical practice. FMRI maps obtained using this approach correlate with intra-operative electrophysiology (Vlieger et al., 2004), electrical stimulation mapping (Mehta and Klein, 2010; Qian et al., 2013), Wada testing (Adcock et al., 2003; Binder et al., 1996; Desmond et al., 1995), and loss-of-function post-operatively (Haberg et al., 2004; Richardson et al., 2004). However, pre-operative mapping patients frequently lack the ability to perform tasks well due to age or disability (Pujol et al., 1998), maps are frequently confounded by artifact (Lee et al., 1999), accuracy and clinical utility can vary widely across patients and studies (Dimou et al., 2013; Giussani et al., 2010), and task-based mapping utilizes only a small percentage of total fMRI variance (Fox et al., 2007; Fox et al., 2006).

A complimentary mapping approach that circumvents some of these limitations assesses correlations in spontaneous brain activity that occurs during rest. Termed resting state functional connectivity (rs-fcMRI), this technique has proven valuable for mapping functional networks including the motor system (Biswal et al., 1995; Fox and Raichle, 2007). Spontaneous activity mapping can be performed when subjects are asleep (Fukunaga et al., 2006; Horovitz et al., 2006) and sedated (Greicius et al., 2008; Kiviniemi et al., 2003; Peltier et al., 2005; Vincent et al., 2007), expanding applicable patient populations. Several articles have recently shown proof of concept for rs-fcMRI as a pre-operative mapping tool in patients with neurosurgical conditions (Kokkonen et al., 2009; Liu et al., 2009; McCormick et al., 2013; Mitchell et al., 2013; Shimony et al., 2009; Zhang et al., 2009). These articles report good correlation between rs-fcMRI results, task-based mapping, and intra-operative cortical stimulation. However, rs-fcMRI is confounded by different but

equally problematic artifacts (Buckner et al., 2013; Fox and Raichle, 2007), and most patients can perform tasks at least partially leading to a reticence to abandon task-based pre-operative mapping in favor of rs-fcMRI.

In theory, one could perform both spontaneous and task-based mapping in the same patients to potentially improve pre-operative functional localization. However, it remains unknown if the two approaches provide independent or redundant information and whether the combination would provide any advantage. Even if beneficial, the combination may not be practical. Performing both types of scans would require a doubling of MRI scan time, an unattractive option from the perspective of cost, patient convenience, and data quality as movement artifact becomes worse the longer patients are in the scanner.

Here we propose a novel processing approach for pre-operative fMRI data based on the concept that the fMRI signal acquired during a task is a superposition of underlying coherent spontaneous activity and task-based modulation (Arfanakis et al., 2000; Fox et al., 2007; Fox et al., 2006; Krienen et al., 2014). Using standard pre-operative mapping fMRI data, we hypothesize that one can separate these two signals, obtain two different spatial maps based on these signals, then combine the maps to get a more robust pre-operative mapping result (see Figure 1). In the current article, we develop this approach and test its performance against direct electrical cortical stimulation (ECS).

MATERIALS AND METHODS

Two independent datasets were included in the present article. The first dataset (eight patients) was used for initial development and testing of our processing algorithm. The second dataset (six patients) was used to prospectively confirm utility in an independent cohort from a different center. Both datasets consisted of patients with intractable epilepsy undergoing pre-surgical workup including a preoperative fMRI scan, surgical implantation of subdural electrode grids, and direct electrical cortical stimulation (ECS) mapping using these grids. In both datasets, electrode grids were placed independent of the functional MRI data and based solely on clinical need.

DATASET 1

Participants—Eight patients (age 19.5 ± 5.0; 3 male) were included. This was a subset of patients from a published study of cortical mapping using gamma-band oscillations recorded from subdural electrode grids (Qian et al., 2013). Detailed demographic information appears in Table S1. No seizures were observed one hour before or after the fMRI or ECS in all patients. Written consent was obtained from each patient or their parents and the experiment was approved by the Ethics Committees of the Second Affiliated Hospital of Tsinghua University.

MRI data acquisition—MRI data was collected on a Philips Achieva 3.0 Tesla TX whole body MR scanner using an 8-channel SENSE head coil. Structural images were acquired using a sagittal magnetization-prepared rapid gradient echo T1-weighted sequence (TR = 8.1 ms, TE = 3.7 ms, TI = 1000 ms, flip angle = 8, FOV = 230 mm × 230 mm, matrix size =230 × 230, slices = 180, voxel size = 1×1×1 mm). Functional data was collected using an echo

planar imaging sequence (TR = 3000 ms, TE = 30 ms, flip angle = 90, FOV = 192 mm×192 mm, matrix size = 64×64, slices = 47, voxel size = 3×3×3 mm).

Two types of functional runs were collected, task activation runs (all eight subjects) and resting state or spontaneous activity runs (six of eight subjects). Task activation runs included self-paced movements of the left hand, right hand, left foot, right foot, or tongue. Each subject completed five task runs, one run for each type of movement. Each task run was 144 seconds long and consisted of six 12-second task blocks interleaved with six 12-second rest intervals. Patients performed motor tasks according to the instructions presented on the computer screen using the Psychophysics Toolbox in MATLAB (The MathWorks, Inc.). A mirror mounted on the head coil enabled subjects to see the screen in the scanner.

Six subjects also underwent two resting-state runs (360s each run), during which they were asked to fixate on a crosshair in the center of the screen. These pure resting state runs were collected for comparison purposes with the maps created based on spontaneous activity extracted from the task runs.

Electrical cortical stimulation data acquisition—All implanted grids had an electrode spacing of 10 mm. After an adequate number of seizures had been recorded, direct electrical cortical stimulation mapping was performed at the bedside to identify motor and somatosensory cortices (Qian et al., 2013). Using an Ojemann Cortical Stimulator (Integra Life- Sciences), trains of 60-Hz biphasic pulses lasting for 2–5 seconds were delivered to selected pairs of electrodes. The current intensity of the stimulation started at 2 mA and was gradually increased until patients showed or reported symptoms related to the sensory motor cortex or the stimulus strength reached 15 mA. As each stimulation involved a pair of electrodes, both electrodes were considered positive when a hand or tongue movement or sensation was produced. If any movement or sensory response was observed at any stimulus strength the electrode was considered “positive” while the lack of any response designated an electrode as “negative”. ECS mapping was not performed for the foot area.

Registering intracranial electrodes to cortical surface and ROI definition—A post-implantation CT scan was obtained within 24–48 h after the implant surgery for localizing the electrodes. The post-implantation CT images were registered to the T1-weighted MRI images with a mutual-information-based linear transform algorithm (Qian et al., 2013). Cortical surfaces were reconstructed from high-resolution T1-weighted images using the Freesurfer 4.5.0 pipeline (Fischl et al., 2002). To facilitate the extraction of electrode coordinates, the 3D pial surface was overlaid with semitransparent CT images using our in-house visualization toolbox. The effects of surgical intervention may cause the exposed brain to move away from the skull and some of the electrodes extracted from post-implantation CT images may appear off the surface reconstructed from pre-surgical MR images. In order to correct this non-linear distortion of the brain surface, these electrodes’ locations were manually adjusted according to the grid shape and other electrodes on the 3D pial surface. This manual adjustment was done prior to the functional MRI data processing and with no knowledge of subsequent functional information.

DATASET 2

Participants—Six patients (age 34 ± 11.0; 1 male) were included in this cohort. This is the first report analyzing preoperative mapping data from this cohort and detailed demographic information is available in supplementary material (Table S1). Participants were recruited through the North Shore-LIJ Comprehensive Epilepsy Center and gave informed consent to contribute these data for research purposes in accordance with a research protocol approved by the local Institutional Review Board. All patients with pharmacologically intractable epilepsy undergoing intracranial electrode implantation as part of their evaluation for epilepsy surgery were candidates for participation in this study.

MRI data acquisition—Prior to electrode implantation, MRI data were acquired on a GE Signa HDx 3T whole-body scanner with an eight-channel head coil. All subjects had a T1-weighted anatomical MRI using a 3D spoiled gradient recalled sequence, although the exact parameters varied. For the first three patients (Sub1–3) the anatomical scan was acquired using axial sections (TR = 7.8 ms, TE = 3.0 ms, TI = 650 ms, flip angle = 8, FOV = 256 mm, matrix = 256×256, slices = 180, voxel size = 1×1×1 mm) while for the remaining three patients the anatomical scan was acquired using sagittal sections (TR = 6.5 ms, TE = 2.8 ms, TI = 600 ms, flip angle = 8, FOV = 240 mm, matrix = 256×256, slices = 170, voxel size = 1.2×0.9×0.9 mm).

Finger tapping functional imaging data were acquired using a gradient echo, echoplanar (EPI) sequence (2000 ms TR, 28 ms TE, 220 mm FOV, 70 degree flip angle, 64×64 matrix size, 4mm thickness, 34 transverse slices, 120 volumes, voxel resolution = 3.4×3.4×4 mm). Patients were asked to tap their fingers against their thumbs with one or both hands for a 30 second block of time followed by 30 seconds of rest. This procedure was repeated four times for a total task time of four minutes. Patients were instructed to tap or rest via instructions presented using text projected onto a mirror mounted on the head coil. These instructions were presented using E-Prime (Psychology Tools, Pittsburgh, PA) on an IFIS-SA system (In-vivo, Orlando, FL). An experimenter observed patient behavior to ensure that they accurately followed instructions.

Electrical stimulation mapping—All electrode grids had 10 mm spacing between electrodes except for one subject (Sub 2) in which some strips / grids with 4 mm spacing were also used. Electrical stimulation mapping was performed with a Grass S-12 Isolated Biphasic Stimulator. Bipolar stimulation was delivered to adjacent electrode pairs according to clinical protocol (50 Hz, 200 ms pulse width, 2–10 sec trains). Current amplitude was manually controlled and ranged from 4 to 8 mA, limited by after-discharge threshold, to find the minimal current necessary to elicit a functional response. Motor areas were identified when stimulation resulted in clonus. Stimulation sites yielding motor or sensory responses of the hand and or tongue were identified and those without such responses were defined as “clear.”

Electrode Localization—To localize electrodes relative to the pre-implant MRIs, all participants received 1 mm axial CT (Siemens Somatom Definition) and 1.5T T1 MRI (GE Signa Excite Scanner) scans within 24–48 hours following electrode implantation. Electrode

locations were manually identified on the CT scan using BioImage Suite (Version 3, http://www.bioimagesuite.org)(Papademetris et al., 2006). These locations were then mapped to the pre-implant MRI via a six degree of freedom affine (i.e., rigid) transformation derived from co-registering the pre-implant MRI and post-implant CT scans to the post-implant MRI scan. All co-registration was done using FSL's FLIRT (Jenkinson and Smith, 2001). The reconstructed pial surface was computed from the pre-implant MRI using FreeSurfer (http://surfer.nmr.mgh.harvard.edu/) and the electrode coordinates projected to the pial surface to correct for possible brain shift caused by electrode implantation and surgery (Dykstra et al., 2012). This pial surface projection method has been shown to produce results that closely correspond with intraoperative photographs with a median disagreement of ~3 mm (Dykstra et al., 2012).

DATA ANALYSIS (BOTH DATASETS)

MRI data analysis—MRI data from both datasets were processed in surface-space using previously described procedures (Wang et al., 2013; Yeo et al., 2011b). Surface mesh representations of the cortex from each individual subject's structural images were reconstructed and registered to a common spherical coordinate system (Fischl et al., 1999). The structural and functional images were aligned using boundary-based registration (Greve and Fischl, 2009). The BOLD fMRI data were then aligned to the common spherical coordinate system via sampling from the middle of the cortical ribbon in a single interpolation step. See (Yeo et al., 2011b) for details.

To facilitate comparison between ECS mapping results and fMRI data, MRI surface vertices within a 6 mm radius of electrodes associated with hand or tongue responses were defined as positive while all other vertices were defined as negative. The 6 mm radius was chosen based on the electrode spacing (10 mm), however results did not differ if one used a 4 mm or 8 mm radius instead (Figure S2). The resulting mask was smoothed with a 6 mm full-width-half-maximum kernel across vertices. This ECS surface map was used to generate hand or tongue regions of interest for the analysis of fMRI signal to noise ratios.

Task Activation Mapping: Conventional task-evoked activation maps for hand and tongue movements were estimated using the general linear model as implemented in SPM2 (Wellcome Department of Cognitive Neurology, London, UK). Regressors of no interest included motion correction parameters and low frequency drift. Task induced BOLD response was modeled by convolving the hemodynamic response function with the experimental design. The significance of the task activation at each vertex was calculated in SPM2 using a t-test. Resulting p values were converted into −log (p) values for visualization and further processing, for example 10^{-6} became 6.

Spontaneous Activity Mapping: Maps based on spontaneous activity were constructed from two sources, residual spontaneous activity underlying task-evoked activity from the task runs (DATASETS 1 and 2) and pure resting state runs that consisted entirely of spontaneous activity (DATASET 1 only). Data were band-passed filtered (0.01–0.08 Hz) and several sources of spurious or regionally nonspecific variance were regressed out. Nuisance regressors included six-parameter rigid body head motion obtained from motion correction,

the signal averaged over the whole brain (the global signal), the signal averaged over the lateral ventricles, and the signal averaged over a region centered in the deep cerebral white matter (Fox et al., 2005; Van Dijk et al.; Yeo et al., 2011b). Because inclusion of the global signal in nuisance regression can be controversial, we repeated our analysis without this processing step (Figure S2). For processing of the task-based data, an extra nuisance regressor was included consisting of the modeled task-related response. This additional regressor removes much of the task-related variance from the task runs, leaving behind spontaneous activity. This procedure has been used previously for estimation of functional connectivity from task data (Fair et al., 2007; He et al., 2007), and includes spontaneous activity throughout the task run, not just from the rest blocks. The data from all five types of movement tasks were concatenated for spontaneous activity analysis.

Functional maps based on spontaneous activity were generated using a parcellation approach that segments the cortex into distinct functional areas based on the correlation of each brain vertex with multiple pre-set regions of interest. A similar approach has been used previously to segment the thalamus into distinct nuclei (Zhang et al., 2008; Zhang et al., 2010). Our pre-set regions of interest consisted 17 regions per hemisphere, or 34 regions total, divided into 8 functional networks (Figure S1). These regions and networks were taken from a previous cortical parcellation study, with the somatomotor network subdivided into separate hand and tongue regions based on the higher order parcellation (Yeo et al., 2011a). For each brain vertex in the diseased hemisphere, correlations to the 17 regions in the opposite healthy hemisphere were calculated. Only cross-hemisphere correlations to the healthy hemisphere were used to render the technique robust to local perturbations in anatomy. These 17 regional correlation values were reduced to 8 network correlation values by averaging the results from multiple regions within a network (see Figure S1). Each vertex was identified as part of the network to which it showed the strongest positive correlation (winner-take-all). The intensity of each vertex within a network is the ratio of the vertex's correlation with that network over the vertex's correlation to the next highest network. As such, voxels with the highest values are those that clearly belong to one network and not other networks. This cortical parcellation approach thus allows hand and tongue maps to be identified for each subject based on spontaneous activity. A parcellation approach was used in favor of the simpler seed-based mapping as preliminary analyses suggested that parcellation was less susceptible to artifact and provided more distinct and reproducible cortical boundaries in individual subjects.

Combo Mapping: The task-evoked activation map and spontaneous activity map produced above were combined into a single functional map using a weighted average. The weighting was allowed to vary across subjects since the robustness of the task activation map is likely to vary based on how well a subject performed the task. The robustness of the task activation map for each subject was quantified by averaging the −log(p) values of the most activated vertices, defined as the vertices where the −log(p) value is more than two standard deviations away from the mean. If the mean −log(p) value of these top vertices was larger than 6, the map was considered robust and the task-evoked and spontaneous activity maps were weighted equally. If the average −log(p) value of the top vertices was above this threshold,

the spontaneous activity map was weighted more heavily than the task activation map according to the following equation.

$$Combo\ Map = \left(1 - \frac{x}{2 \times th}\right) \times Spontaneous\ Activity\ Map + \frac{x}{2 \times th} \times Task\ Activation\ Map$$

where x is the mean $-log(p)$ values of the top vertices and th is the threshold. In our data, we used a threshold of $-log(p) = 6$. Note that in the limiting case where subjects are unable to perform the task, the combo map would become identical to the spontaneous activity map. Because the task activation map and spontaneous activity map are based on different scales, both were normalized to a maximum value of 1 by dividing all vertices by the value of the peak vertex prior to combining the maps.

Signal to Noise Calculation for fMRI data—To compare signal to noise ratios between processing approaches, we extracted fMRI time courses from ECS-defined hand and tongue ROIs after the fMRI data had been corrected for linear drift and movement. Signal was defined as the amount of fMRI variance utilized in computing a given map while noise was any residual variance not utilized in map creation (Fox et al., 2007; Fox et al., 2006). Variance utilized in task activation mapping was computed based on the hemodynamically convolved task model. Variance utilized in spontaneous activity mapping was computed as variance of spontaneous activity multiplied by the square of the correlation coefficient between the regional timecourse and the somatomotor ROI in the opposite hemisphere. Differences in signal to noise ratio between mapping strategies was compared using a Wilcoxon paired non-parametric test.

Comparing the task fMRI and combo fMRI mapping with ECS findings—Results of different mapping modalities were projected to each individual's brain surface for the comparison with the ECS findings. Taking the ECS findings as the reference, sensitivity and specificity of the activation map and combo map were quantified. Results for tongue and hand in DATASET1 were combined within a subject. Sensitivity was computed by dividing the number of true positives (fMRI positive vertices that were also positive by ECS) by the number of true positives plus false negatives (i.e. total vertices positive by ECS). The specificity was computed by the number of true negatives (fMRI negative vertices that were also negative by ECS) divided by the number of true negatives plus false positives (i.e. total vertices negative by ECS). Receiver operating characteristic (ROC) curves were obtained by calculating the sensitivity and specificity across a wide range of different thresholds. These ROC curves were constructed for each subject individually. The area under the curve was computed for each subject and compared across methods using a Wilcoxon paired non-parametric test. Numerical values in the text and tables reflect these single-subject measurements, or the average across these single subject measurements, and are the values upon which all statistical comparisons were made. However, for display purposes group-level ROC curves were also constructed for each method, combining data across all subjects within a dataset. These group-level ROC curves provide a useful graphical illustration of the benefit of one method relative to another, but cannot be used for statistical comparisons.

Alternative Approaches—In addition to the combo mapping approach detailed above, we also tested several alternative approaches to combination mapping and compared their performance to that of our primary analysis. These alternative approaches were all tested using DATASET 1.

1) Anatomical Weighting: Rather than combine task activation maps with spontaneous activity maps, the task activation map could be combined with anatomical information to improve accuracy. This approach is similar to the mental process many clinicians use when viewing conventional pre-operative fMRI maps; greater emphasis is placed on activations close to the expected anatomical location than those distant from it. Two anatomical weighting approaches were used. In the first approach, the automatic anatomical parcellation generated by Freesurfer surface registration was used as subject-specific masks of the pre- and post-central gyri. In the second approach, the putative hand and tongue seed regions obtained by the functional connectivity analysis as described in (Yeo et al., 2011b) (see Figure S1) were employed as anatomical masks. In each case, hybrid maps were produced by masking the task activation maps with anatomical maps. As the accuracy of this approach can depend on the accuracy of the anatomical parcellation, this analysis was repeated after excluding subjects with any anatomical distortion (see Figure S3).

2) True resting state data: In six of eight subjects data pure resting state data was collected for comparison with spontaneous activity extracted from the task runs. As in the main analysis described above, the same weighting algorithm was used, but with spontaneous activity parcellation maps generated based on true resting state data from each subject. This analysis provides information regarding whether there is benefit to acquiring separate resting state and task activation scans to generate the two maps or whether both maps can be generated using the same task-based dataset as proposed here.

For all of these alternative combo mapping strategies, ROC curves were generated and the area under the curve was compared with that of our primary combo mapping analysis.

RESULTS

All initial analyses were performed using DATASET 1, then key results were confirmed in DATASET 2. In the motor regions of interest defined by ECS, task-related activity accounted for 32.5% of the total variance in the BOLD signal. In traditional task activation mapping, the rest of the BOLD variance including coherent spontaneous activity is discarded as noise. In the combo mapping approach, underlying coherent spontaneous activity that persists throughout the task run is used as an additional signal for functional mapping along with the task-related activity. On average, combo mapping results in a 43.2% increase in signal to noise ratio ($p < 0.001$) compared to the conventional task activation approach (Table S2).

Next, we determined whether this improvement in signal to noise ratio translated into more accurate pre-operative maps, using electrical cortical stimulation as our standard (Figure 2). Conventional task activation maps often implicated regions outside the sensorimotor strip including portions of the temporal and occipital lobes. Combining the task–activation map

with the map based on underlying spontaneous activity appeared to improve specificity and correspondence to results obtained with cortical stimulation across all eight subjects.

To compare the performance of combo mapping with traditional task activation mapping independent of threshold, we constructed ROC curves for each individual subject as well as a single ROC curve for the entire group (Figure 3). ROC curves indicate the sensitivity and specificity of a technique across different thresholds. For example, if one were to threshold maps for a specificity of 80% combo mapping would improve sensitivity from 62% to 82% compared to task activation mapping. If one were to threshold for a sensitivity of 70%, combo mapping would increase specificity from 71% to 95% compared to task activation mapping. A larger area under the curve (AUC) indicates a more sensitive and specific technique across all thresholds. Combo mapping showed a significant improvement over conventional task activation mapping (AUC of 0.882 vs 0.767, $p < 0.01$) (Figure 3, see also Table S3). Note that this improvement came from the combination of the two mapping approaches, not just the accuracy of the spontaneous activity map alone, as the combo map performed significantly better than spontaneous activity by itself (AUC of 0.882 vs 0.757, $p < 0.01$; Figure 4).

Although combo mapping showed significant improvement across all subjects, some subjects showed more improvement than others (Table S2, S3). Subjects that showed the greatest improvement in signal to noise also showed the largest improvement in AUC ($r = 0.92$, $p < 0.005$) providing a nice internal validation of the two metrics. Much of this inter-subject variability can be attributed to differences in the quality of the initial task activation map. Subjects that showed the greatest improvement with combo mapping were the ones that showed the weakest task activation, measured by either signal to noise ($r = -0.76$, $p < 0.05$) or AUC ($r = -0.82$, $p < 0.005$).

An important question is whether the spontaneous activity mapping is contributing anything to the combo map beyond simple anatomical weighting. We recomputed combo maps based on anatomical weighting (see methods). The anatomy-weighted combo map showed some improvement in AUC (0.812 for Freesurfer anatomical parcellation and 0.823 for pre-determined seeds) beyond the conventional task activation approach ($p < 0.01$ for both approaches), but was significantly worse than our main combo mapping approach using underlying spontaneous activity ($p < 0.01$ for both approaches) (Figure 4, see also Table S3). To ensure this was not due to poor anatomical parcellation, we examined anatomical results for each subject (Figure S3) and excluded subjects with anatomical distortion. Combo mapping continued to outperform anatomical weighting (AUC 0.879 vs 0.822, $p < 0.05$). Finally, we asked whether adding anatomical weighting to our combo mapping approach would further improve the technique, and the change was insignificant (AUC 0.882 vs 0.878, $p > 0.3$).

Another important question is whether combo mapping would be even better if one used a dedicated resting state fMRI scan to compute the spontaneous activity map rather than the spontaneous activity underlying the task-based signal. Although the ROC curve was slightly better using a dedicated resting state scan, the difference was small and not significant (AUC 0.882 vs 0.905, $p > 0.15$) (Figure 4, see also Table S3). We also investigated whether global

signal regression made a difference in the accuracy of our approach, and although there was no significant difference our approach performed slightly better with global signal regression than without (Figure S2, AUC 0.882 vs 0.851, $p > 0.2$).

Finally, we tested whether our results would replicate across other centers, MRI machines, and patient cohorts. We prospectively validated our processing algorithm using an independent cohort of 6 patients, again using ECS mapping to assess the accuracy of the fMRI results. Results were similar and in fact showed even greater improvement than observed in our initial cohort. Compared to the conventional processing approach, our combo mapping algorithm improved signal to noise ratio by a factor of eight and significantly improved the sensitivity and specificity of fMRI mapping (AUC 0.856 vs 0.643, $p < 0.01$) (Figure 5, Table S4, Table S5).

DISCUSSION

Here we present a novel approach for processing pre-operative fMRI data that greatly improves signal to noise, sensitivity, and specificity, compared to the conventional processing approach. These results provide insight into the relationship between spontaneous and task-evoked activity and have potential implications for improving clinical practice.

Our technique is based on the premise that the fMRI signal recorded during a task paradigm is composed of task-based modulation and underlying coherent spontaneous activity, and that both provide information useful for functional mapping. Prior work has shown that coherent spontaneous activity doesn't disappear during task paradigms, but continues (Arfanakis et al., 2000; Fox et al., 2007; Fox et al., 2006). To a rough approximation, there is a linear superposition between task-evoked and spontaneous activity (Arieli et al., 1996; Fox et al., 2006), although some interaction between these two types of activity does occur (Fox et al., 2007; He, 2013; Nir et al., 2006). Only the task-evoked component has routinely been used for functional mapping, however one can generate maps based on the spontaneous activity underlying the task-evoked activity (Fair et al., 2007), and it has been hypothesized that this might be useful for pre-operative mapping (Zhang et al., 2009). Nevertheless it was unknown whether maps generated using underlying spontaneous activity contained any useful information for functional localization beyond the information already available from task-evoked maps. It was also unknown whether this additional information would be better or worse than information obtained from anatomy or "pure" spontaneous activity recorded during independent resting state scans. To our knowledge, this is the first study to examine these questions, in part because answering them requires patient cohorts that have both pre-operative fMRI and electrophysiological mapping data allowing for validation and quantitative comparison between different fMRI results.

In the pre-operative fMRI literature, imaging results are frequently related to intra-operative direct electrical cortical stimulation (ECS) as a gold standard. However the correspondence between the two techniques is often reported qualitatively and finding metrics to address this quantitatively has been challenging (Vlieger et al., 2004). One approach is to measure the distance between the center of fMRI and ECS localizations (Kapsalakis et al., 2012),

however the extent is likely as important as the center when the goal is to avoid postoperative deficits. Other studies have reported the number of ECS points that fall within the activated area of fMRI, however this is critically dependent on the threshold used to differentiate “activated” from “non-activated” voxels and the spatial locations of ECS-negative points are often not recorded (Vlieger et al., 2004). In the current study, we utilized somewhat unique datasets where the spatial location of both positive and negative ECS electrodes was well characterized. Further, we used ROC analysis to assess sensitivity and specificity independent of threshold (Park et al., 2004). The use of ROC curves in evaluating the sensitivity and specificity of preoperative fMRI mapping allows us to characterize that utility of different mapping approaches with high accuracy (FitzGerald et al., 1997; Kunii et al., 2011; Mitchell et al., 2013).

An important feature of our fMRI processing algorithm is that it requires no additional tasks or scan time to improve functional localization. Other approaches such as adding additional tasks (Ramsey et al., 2001) or performing separate task and rest scans (Kokkonen et al., 2009; Liu et al., 2009; Shimony et al., 2009; Zhang et al., 2009) may be limited by these practical considerations. Interestingly, we found little benefit to performing separate task and rest runs compared to extracting underlying spontaneous activity from the task data. The amount of pure rest data (2 runs × 360 seconds = 720) was identical to the amount of data from the task runs (5 runs × 144 seconds = 720). This is important as it suggests that our combo mapping approach performs well when only task data is available. However, this analysis was based on only six subjects, and if time and resources permit there may be some advantage to dedicated rest runs (Fair et al., 2007). This question should be readdressed in larger cohorts with greater statistical power.

An interesting aspect of our study is the comparison with anatomical weighting. Although the focus of this study was on combining task activation with underlying spontaneous activity, the combination of task activation and anatomical weighting also improved results beyond task activation alone. This improvement was not as robust as using spontaneous activity, however future improvements in anatomical registration and parcellation such as myelin mapping may prove valuable (Glasser and Van Essen, 2011; Robinson et al., 2014).

A major strength of our study is the use of two independent datasets from different centers, different MRI scanners, and different pre-operative mapping paradigms. Some fMRI processing parameters were adjusted for optimal performance on DATASET 1, however these parameters were all held constant when the algorithm was prospectively validated on DATASET 2. The consistency of our results across datasets and the fact that our approach improved individualized fMRI mapping accuracy in each of the fourteen patients examined suggests that our processing approach will be broadly applicable. However, there are still limitations. First, both datasets consisted exclusively of patients with intractable epilepsy. This patient population was selected because their implanted electrode grids allow for comprehensive electrophysiological mapping necessary for ROC analysis and quantification of fMRI results. Our technique remains to be tested in other patient populations such as those undergoing pre-operative fMRI for tumor resection or those in which fMRI scanning is difficult such as children or patients with cognitive impairment. That said, there is reason to believe that our algorithm will perform well in other patient groups. First, the algorithm is

designed to adjust to varying levels of ability to perform the task, defaulting to complete spontaneous activity mapping in a patient with no task activation. This is an advantage for impaired patient populations or children in whom predicting task compliance a priori may be difficult. Second, our spontaneous activity mapping is only dependent on correlations assessed with remote regions of interest, in this case in the opposite hemisphere. This should make the algorithm robust to local disturbances in anatomy like brain tumors, and in fact the algorithm performed well in one of our patients in who epilepsy was due to a large frontal brain tumor (subject 3, DATASET2).

Another limitation of the current study is that it was restricted to mapping of eloquent motor cortex and not tested for other functions such as language or memory. This choice was intentional as localization of eloquent motor cortex with ECS is reasonably straightforward, providing a solid electrophysiological standard against which we could validate our fMRI technique. Mapping functions such as language or memory with ECS is much more complicated, with no clear consensus on what constitutes functional disruption versus sparing (Giussani et al., 2010; Hamberger, 2007). Now that our technique is validated with motor mapping, there is good motivation to begin testing it for language and memory. Pre-operative fMRI mapping of these functions tends to be less robust than motor mapping and thus there is greater need for improvement (Hirsch et al., 2000; Kapsalakis et al., 2012; Mehta and Klein, 2010). Further, there is good reason to think our algorithm will prove useful in these other domains. Similar to the somatomotor system, language and memory systems have been mapped using spontaneous activity recorded with fMRI (McCormick et al., 2013; Tie et al., 2013; Vincent et al., 2006). There is no reason to think that incorporation of spontaneous activity into preoperative mapping will be any less useful for these other systems. Also, our combo mapping algorithm showed the greatest benefit in patients with the poorest task activation. This suggests that language or memory mapping, which generally produce weaker activation maps, could benefit even more from combo mapping than localization of somatomotor cortex.

There are a few additional limitations in this study that deserve mention. First, our ROC analysis in each patient was restricted to the area of the brain covered by the electrode grid. This means that mouth or tongue areas were not fully covered in all patients (e.g. subject 4 and 8, Figure 2). Second, ECS was used as an electrophysiological “gold” standard upon which to validate and compare our fMRI results, however ECS itself not a perfect technique. For example, in one patient ECS mapping failed to identify a likely tongue area identified on fMRI (subject 5, Figure 2). Future work using post-operative deficits as an outcome measure will be important. Third, our combo mapping algorithm relied on an empirically derived p-value to determine the “robustness” of an activation map and the weighting to be used when combining it with the spontaneous activity map. We chose a p value of 10^{-6} based on DATASET 1, and this cutoff performed well in DATASET 2. However this value may vary when attempting to map different functions. Future work could parametrically vary this value and the weighting algorithm to establish the best way to combine maps.

Finally, there are limitations to pre-operative fMRI in general that are not addressed by the current algorithm. First, motion is a problem for both task activation and spontaneous activity mapping and improved algorithms for motion correction would be valuable. Second,

registration issues due to intraoperative brain shift can reduce the utility of pre-operative maps in the OR, however intraoperative MRI may help address this problem. Third, the fMRI signal is a hemodynamic correlate of neuronal activity and can therefore bias results towards draining veins or prove unreliable if neurovascular coupling is altered by medications or pathology (Dimou et al., 2013; Vlieger et al., 2004). Finally, fMRI identifies brain areas that correlate with function, but cannot demonstrate whether a region is necessary for function.

CONCLUSION

By utilizing both the task-based and underlying spontaneous activity components of standard preoperative fMRI data from neurosurgical patients we have developed a method to significantly improve the signal to noise ratio, sensitivity, and specificity of preoperative fMRI maps. Because the processing algorithm requires no modification to standard MRI acquisition protocols it may find widespread utility.

Supplementary Material

Refer to Web version on PubMed Central for supplementary material.

Acknowledgments

We thank Abraham Snyder, Marcus Raichle, and Joshua Shimony for early discussions on this concept. MDF is listed as inventor on submitted or issued patents on guiding noninvasive brain stimulation with fMRI. HL, DW, and MDF are listed as inventors on submitted patents on mapping functional brain organization using fMRI. MDF was supported by NIH grants R25NS065743, K23NS083741, the American Brain Foundation, and the Sidney Baer Foundation. HL was supported by NIH grants K25NS069805, R01NS091604, P50 MH106435, and NARSAD Young Investigator Grant.

References

Adcock JE, Wise RG, Oxbury JM, Oxbury SM, Matthews PM. Quantitative fMRI assessment of the differences in lateralization of language-related brain activation in patients with temporal lobe epilepsy. Neuroimage. 2003; 18:423–438. [PubMed: 12595196]

Arfanakis K, Cordes D, Haughton VM, Moritz CH, Quigley MA, Meyerand ME. Combining independent component analysis and correlation analysis to probe interregional connectivity in fMRI task activation datasets. Magnetic Resonance Imaging. 2000; 18:921–930. [PubMed: 11121694]

Arieli A, Sterkin A, Grinvald A, Aertsent A. Dynamics of ongoing activity: explanation of the large variability in evoked cortical responses. Science. 1996; 273:1868–1871. [PubMed: 8791593]

Binder JR, Swanson SJ, Hammeke TA, Morris GL, Mueller WM, Fischer M, Benbadis S, Frost JA, Rao SM, Haughton VM. Determination of language dominance using functional MRI: a comparison with the Wada test. Neurology. 1996; 46:978–984. [PubMed: 8780076]

Biswal B, Yetkin FZ, Haughton VM, Hyde JS. Functional connectivity in the motor cortex of resting human brain using echo-planar MRI. Magn Reson Med. 1995; 34:537–541. [PubMed: 8524021]

Buckner RL, Krienen FM, Yeo BT. Opportunities and limitations of intrinsic functional connectivity MRI. Nature Neuroscience. 2013; 16:832–837. [PubMed: 23799476]

Desmond JE, Sum JM, Wagner AD, Demb JB, Shear PK, Glover GH, Gabrieli JD, Morrell MJ. Functional MRI measurement of language lateralization in Wada-tested patients. Brain : a journal of neurology. 1995; 118(Pt 6):1411–1419. [PubMed: 8595473]

Dimou SS, Battisti RAR, Hermens DFD, Lagopoulos JJ. A systematic review of functional magnetic resonance imaging and diffusion tensor imaging modalities used in presurgical planning of brain tumour resection. Neurosurgical Review. 2013; 36:205–214. [PubMed: 23187966]

Dykstra AR, Chan AM, Quinn BT, Zepeda R, Keller CJ, Cormier J, Madsen JR, Eskandar EN, Cash SS. Individualized localization and cortical surface-based registration of intracranial electrodes. Neuroimage. 2012; 59:3563–3570. [PubMed: 22155045]

Fair DA, Schlaggar BL, Cohen AL, Miezin FM, Dosenbach NU, Wenger KK, Fox MD, Snyder AZ, Raichle ME, Petersen SE. A method for using blocked and event-related fMRI data to study "resting state" functional connectivity. Neuroimage. 2007; 35:396–405. [PubMed: 17239622]

Fischl B, Salat DH, Busa E, Albert M, Dieterich M, Haselgrove C, Van Der Kouwe A, Killiany R, Kennedy D, Klaveness S. Whole brain segmentation: automated labeling of neuroanatomical structures in the human brain. Neuron. 2002; 33:341–355. [PubMed: 11832223]

Fischl B, Sereno MI, Dale AM. Cortical surface-based analysis. II: Inflation, flattening, and a surface-based coordinate system. Neuroimage. 1999; 9:195–207. [PubMed: 9931269]

FitzGerald DB, Cosgrove GR, Ronner S, Jiang H, Buchbinder BR, Belliveau JW, Rosen BR, Benson RR. Location of language in the cortex: a comparison between functional MR imaging and electrocortical stimulation. American Journal of Neuroradiology. 1997; 18:1529–1539. [PubMed: 9296196]

Fox MD, Raichle ME. Spontaneous fluctuations in brain activity observed with functional magnetic resonance imaging. Nat Rev Neurosci. 2007; 8:700–711. [PubMed: 17704812]

Fox MD, Snyder AZ, Vincent JL, Corbetta M, Van Essen DC, Raichle ME. The human brain is intrinsically organized into dynamic, anticorrelated functional networks. PNAS. 2005; 102:9673–9678. [PubMed: 15976020]

Fox MD, Snyder AZ, Vincent JL, Raichle ME. Intrinsic fluctuations within cortical systems account for intertrial variability in human behavior. Neuron. 2007; 56:171–184. [PubMed: 17920023]

Fox MD, Snyder AZ, Zacks JM, Raichle ME. Coherent spontaneous activity accounts for trial-to-trial variability in human evoked brain responses. Nature Neuroscience. 2006; 9:23–25. [PubMed: 16341210]

Fukunaga M, Horovitz SG, Van Gelderen P, de Zwart JA, Jansma JM, Ikonomidou VN, Chu R, Deckers RHR, Leopold DA, Duyn JH. Large-amplitude, spatially correlated fluctuations in BOLD fMRI signals during extended rest and light sleep. Magnetic Resonance Imaging. 2006; 24:979–992. [PubMed: 16997067]

Giussani CC, Roux FEF, Ojemann JJ, Pietro EP Sganzerla E, Pirillo DD, Papagno CC. Is preoperative functional magnetic resonance imaging reliable for language areas mapping in brain tumor surgery? Review of language functional magnetic resonance imaging and direct cortical stimulation correlation studies. Neurosurgery. 2010; 66:113–120. [PubMed: 19935438]

Glasser MF, Van Essen DC. Mapping human cortical areas in vivo based on myelin content as revealed by T1- and T2-weighted MRI. Journal of Neuroscience. 2011; 31:11597–11616. [PubMed: 21832190]

Greicius MD, Kiviniemi V, Tervonen O, Vainionpaa V, Alahuhta S, Reiss AL, Menon V. Persistent default-mode network connectivity during light sedation. Hum Brain Mapp. 2008; 29:839–847. [PubMed: 18219620]

Greve DN, Fischl B. Accurate and robust brain image alignment using boundary-based registration. Neuroimage. 2009; 48:63–72. [PubMed: 19573611]

Haberg A, Kvistad KA, Unsgard G, Haraldseth O. Preoperative blood oxygen level-dependent functional magnetic resonance imaging in patients with primary brain tumors: clinical application and outcome. Neurosurgery. 2004; 54:902–914. discussion 914–905. [PubMed: 15046657]

Hamberger MJ. Cortical language mapping in epilepsy: a critical review. Neuropsychology Review. 2007; 17:477–489. [PubMed: 18004662]

He BJ. Spontaneous and task-evoked brain activity negatively interact. Journal of Neuroscience. 2013; 33:4672–4682. [PubMed: 23486941]

He BJ, Snyder AZ, Vincent JL, Epstein A, Shulman GL, Corbetta M. Breakdown of functional connectivity in frontoparietal networks underlies behavioral deficits in spatial neglect. Neuron. 2007; 53:905–918. [PubMed: 17359924]

Hirsch J, Ruge MI, Kim KH, Correa DD, Victor JD, Relkin NR, Labar DR, Krol G, Bilsky MH, Souweidane MM, DeAngelis LM, Gutin PH. An integrated functional magnetic resonance imaging procedure for preoperative mapping of cortical areas associated with tactile, motor, language, and visual functions. Neurosurgery. 2000; 47:711–712. [PubMed: 10981759]

Horovitz, SG.; Fukunaga, M.; de Zwart, JA.; Van Gelderen, P.; Fulton, SC.; Balkin, TJ.; Duyn, JH. The default-mode network connectivity during awake and early sleep,: A simultaneous EEG-BOLD-fMRI study. Organization for Human Brain Mapping Annual Meeting; Florence, Italy. 2006. p. 686M–PM

Jack CR, Thompson RM, Butts RK, Sharbrough FW, Kelly PJ, Hanson DP, Riederer SJ, Ehman RL, Hangiandreou NJ, Cascino GD. Sensory motor cortex: correlation of presurgical mapping with functional MR imaging and invasive cortical mapping. Radiology. 1994; 190:85–92. [PubMed: 8259434]

Jenkinson M, Smith S. A global optimisation method for robust affine registration of brain images. Med Image Anal. 2001; 5:143–156. [PubMed: 11516708]

Kapsalakis IZ, Kapsalaki EZ, Gotsis ED, Verganelakis D, Toulas P, Hadjigeorgiou G, Chung I, Fezoulidis I, Papadimitriou A, Robinson JS, Lee GP, Fountas KN. Preoperative evaluation with FMRI of patients with intracranial gliomas. Radiology Research and Practice. 2012; 2012:727810–727810. [PubMed: 22848821]

Kiviniemi V, Kantola JH, Jauhiainen J, Hyvarinen A, Tervonen O. Independent component analysis of nondeterministic fMRI signal sources. Neuroimage. 2003; 19:253–260. [PubMed: 12814576]

Kokkonen SM, Nikkinen J, Remes J, Kantola J, Starck T, Haapea M, Tuominen J, Tervonen O, Kiviniemi V. Preoperative localization of the sensorimotor area using independent component analysis of resting-state fMRI. Magn Reson Imaging. 2009; 27:733–740. [PubMed: 19110394]

Krienen FM, Yeo BTT, Buckner RL. Reconfigurable task-dependent functional coupling modes cluster around a core functional architecture. Philosophical Transactions of the Royal Society B: Biological Sciences. 2014; 369

Kunii N, Kamada K, Ota T, Kawai K, Saito N. A detailed analysis of functional magnetic resonance imaging in the frontal language area: a comparative study with extraoperative electrocortical stimulation. Neurosurgery. 2011; 69:590–597. [PubMed: 21430585]

Lee CC, Ward HA, Sharbrough FW, Meyer FB, Marsh WR, Raffel C, So EL, Cascino GD, Shin C, Xu Y, Riederer SJ, Jack CR Jr. Assessment of functional MR imaging in neurosurgical planning. AJNR Am J Neuroradiol. 1999; 20:1511–1519. [PubMed: 10512239]

Liu H, Buckner RL, Talukdar T, Tanaka N, Madsen JR, Stufflebeam SM. Task-free presurgical mapping using functional magnetic resonance imaging intrinsic activity. J Neurosurg. 2009; 111:746–754. [PubMed: 19361264]

Matthews PM, Honey GD, Bullmore ET. Applications of fMRI in translational medicine and clinical practice. Nat Rev Neurosci. 2006; 7:732–744. [PubMed: 16924262]

McCormick C, Quraan M, Cohn M, Valiante TA, McAndrews MP. Default mode network connectivity indicates episodic memory capacity in mesial temporal lobe epilepsy. Epilepsia. 2013; 54:809–818. [PubMed: 23360362]

Mehta AD, Klein G. Clinical utility of functional magnetic resonance imaging for brain mapping in epilepsy surgery. Epilepsy Research. 2010; 89:126–132. [PubMed: 20211545]

Mitchell TJ, Hacker CD, Breshears JD, Szrama NP, Sharma M, Bundy DT, Pahwa M, Corbetta M, Snyder AZ, Shimony JS, Leuthardt EC. A novel data-driven approach to preoperative mapping of functional cortex using resting-state functional magnetic resonance imaging. Neurosurgery. 2013; 73:969–963. [PubMed: 24264234]

Nir Y, Hasson U, Levy I, Yeshurun Y, Malach R. Widespread functional connectivity and fMRI fluctuations in human visual cortex in the absence of visual stimulation. Neuroimage. 2006; 30:1313–1324. [PubMed: 16413791]

Papademetris X, Jackowski MP, Rajeevan N, DiStasio M, Okuda H, Constable RT, Staib LH. BioImage Suite: An integrated medical image analysis suite: An update. Insight J. 2006; 2006:209. [PubMed: 25364771]

Park SH, Goo JM, Jo CH. Receiver operating characteristic (ROC) curve: practical review for radiologists. Korean journal of radiology : official journal of the Korean Radiological Society. 2004; 5:11–18.

Peltier SJ, Kerssens C, Hamann SB, Sebel PS, Byas-Smith M, Hu X. Functional connectivity changes with concentration of sevoflurane anaesthesia. Neuroreport. 2005; 16:285–288. [PubMed: 15706237]

Pujol J, Conesa G, Deus J, Lopez-Obarrio L, Isamat F, Capdevila A. Clinical application of functional magnetic resonance imaging in presurgical identification of the central sulcus. J Neurosurg. 1998; 88:863–869. [PubMed: 9576255]

Qian T, Zhou W, Ling Z, Gao S, Liu H, Hong B. Fast presurgical functional mapping using task-related intracranial high gamma activity. Journal of neurosurgery. 2013; 119:26–36. [PubMed: 23600935]

Ramsey NF, Sommer I, Rutten GJ, Kahn RS. Combined Analysis of Language Tasks in fMRI Improves Assessment of Hemispheric Dominance for Language Functions in Individual Subjects. Neuroimage. 2001; 13:719–733. [PubMed: 11305899]

Richardson MP, Strange BA, Thompson PJ, Baxendale SA, Duncan JS, Dolan RJ. Pre-operative verbal memory fMRI predicts post-operative memory decline after left temporal lobe resection. Brain : a journal of neurology. 2004; 127:2419–2426. [PubMed: 15459025]

Robinson EC, Jbabdi S, Glasser MF, Andersson J, Burgess GC, Harms MP, Smith SM, Van Essen DC, Jenkinson M. MSM: a new flexible framework for Multimodal Surface Matching. Neuroimage. 2014; 100:414–426. [PubMed: 24939340]

Shimony JS, Zhang D, Johnston JM, Fox MD, Roy A, Leuthardt EC. Resting-state spontaneous fluctuations in brain activity: a new paradigm for presurgical planning using fMRI. Acad Radiol. 2009; 16:578–583. [PubMed: 19345899]

Tie Y, Rigolo L, Norton IH, Huang RY, Wu W, Orringer D, Mukundan S, Golby AJ. Defining language networks from resting-state fMRI for surgical planning-a feasibility study. Human Brain Mapping. 2013

Van Dijk KR, Hedden T, Venkataraman A, Evans KC, Lazar SW, Buckner RL. Intrinsic functional connectivity as a tool for human connectomics: theory, properties, and optimization. J Neurophysiol. 103:297–321. [PubMed: 19889849]

Vincent JL, Patel GH, Fox MD, Snyder AZ, Baker JT, Van Essen DC, Zempel JM, Snyder LH, Corbetta M, Raichle ME. Intrinsic functional architecture in the anesthetized monkey brain. Nature. 2007; 447:83–86. [PubMed: 17476267]

Vincent JL, Snyder AZ, Fox MD, Shannon BJ, Andrews JR, Raichle ME, Buckner RL. Coherent spontaneous activity identifies a hippocampal-parietal memory network. J Neurophysiol. 2006; 96:3517–3531. [PubMed: 16899645]

Vlieger EJ, Majoie CB, Leenstra S, Den Heeten GJ. Functional magnetic resonance imaging for neurosurgical planning in neurooncology. Eur Radiol. 2004; 14:1143–1153. [PubMed: 15148622]

Wang D, Buckner RL, Liu H. Cerebellar Asymmetry and Its Relation to Cerebral Asymmetry Estimated by Intrinsic Functional Connectivity. Journal of Neurophysiology. 2013; 109:46–57. [PubMed: 23076113]

Yeo BT, Krienen FM, Sepulcre J, Sabuncu MR, Lashkari D, Hollinshead M, Roffman JL, Smoller JW, Zollei L, Polimeni JR, Fischl B, Liu H, Buckner RL. The Organization of the Human Cerebral Cortex Estimated By Functional Connectivity. Journal of Neurophysiology. 2011a; 106:1125–1165. [PubMed: 21653723]

Yeo BT, Krienen FM, Sepulcre J, Sabuncu MR, Lashkari D, Hollinshead M, Roffman JL, Smoller JW, Zollei L, Polimeni JR, Fischl B, Liu H, Buckner RL. The organization of the human cerebral cortex estimated by intrinsic functional connectivity. J Neurophysiol. 2011b; 106:1125–1165. [PubMed: 21653723]

Zhang D, Johnston JM, Fox MD, Leuthardt EC, Grubb RL, Chicoine MR, Smyth MD, Snyder AZ, Raichle ME, Shimony JS. Preoperative sensorimotor mapping in brain tumor patients using spontaneous fluctuations in neuronal activity imaged with functional magnetic resonance imaging: initial experience. Neurosurgery. 2009; 65:226–236. [PubMed: 19934999]

Zhang D, Snyder AZ, Fox MD, Sansbury MW, Shimony JS, Raichle ME. Intrinsic functional relations between human cerebral cortex and thalamus. J Neurophysiol. 2008; 100:1740–1748. [PubMed: 18701759]

Zhang D, Snyder AZ, Shimony JS, Fox MD, Raichle ME. Noninvasive functional and structural connectivity mapping of the human thalamocortical system. Cereb Cortex. 2010; 20:1187–1194. [PubMed: 19729393]

Highlights

- A new algorithm improves the accuracy of pre-operative fMRI mapping
- The algorithm combines task activations with underlying spontaneous activity
- No additional scan time or specialized sequences are needed
- The algorithm works on data from different patients, MRI scanners, and centers

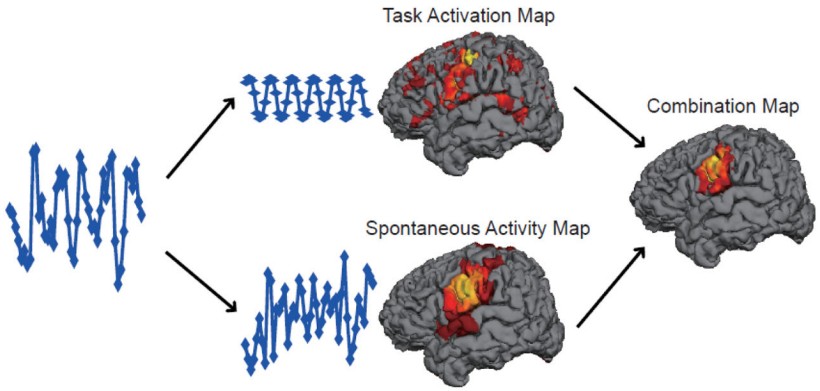

Figure 1.

Methodological approach for combo mapping. Raw BOLD signal obtained from the left motor cortex during tongue movement is extracted (left panel) and decomposed into task-related variance (middle panel, top) and residual spontaneous variance (middle panel, bottom). The task-related variance is used to generate a conventional task activation map (middle panel, top) while the residual spontaneous variance is used to generate a functional connectivity map (middle panel, bottom). The task-based map and spontaneous activity map are combined in a weighted fashion to generate a combo map (right panel).

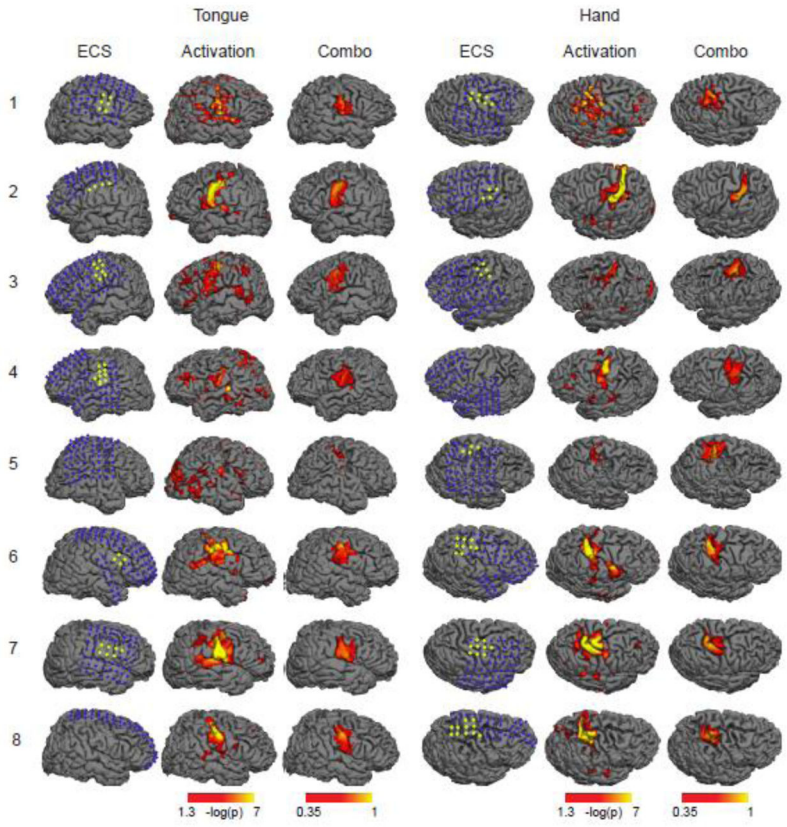

Figure 2.

Tongue and hand motor areas localized by electrical cortical stimulation (ECS), traditional task activation fMRI (Activation), and our novel combo mapping algorithm (Combo) in all eight patients from DATASET 1. The three columns on the left illustrate the tongue regions while the three columns on the right are for the hand regions. The blue dots in the ECS maps indicate negative electrodes (no symptoms related to sensory or motor cortex when stimulated) and the yellow dots indicate positive electrodes. Display thresholds for task activation maps ($-\log(p) = 1.3$) and the combo maps ($i = 0.35$) were selected to correspond to the same sensitivity (60%) with respect to the cortical stimulation results. Compared to the task fMRI results, the combo maps are more consistent with the ECS findings.

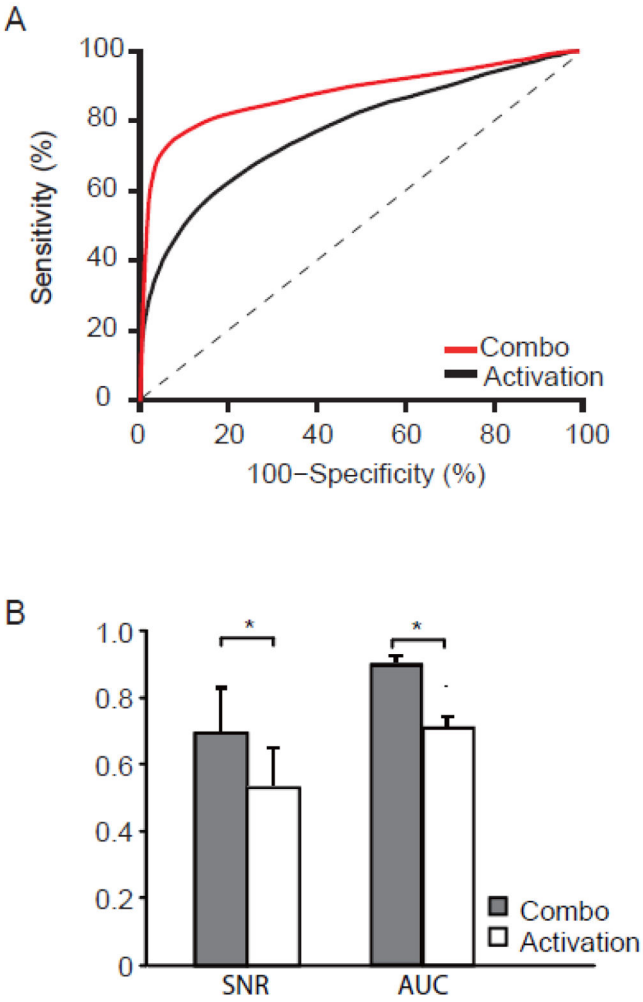

Figure 3.

Combo mapping improves signal to noise and better matches electrical stimulation results compared to traditional task activation mapping. Group-level receiver operating characteristic (ROC) curves show improved sensitivity and specificity of the new combo mapping approach (red curve) compared to traditional task activation mapping approach (black curve) independent of threshold (A). Averaging across single-subject results shows a significant improvement in signal to noise ratio (SNR) and area under the ROC curve (AUC) for combo mapping compared to traditional task activation mapping (B). * $p < 0.01$

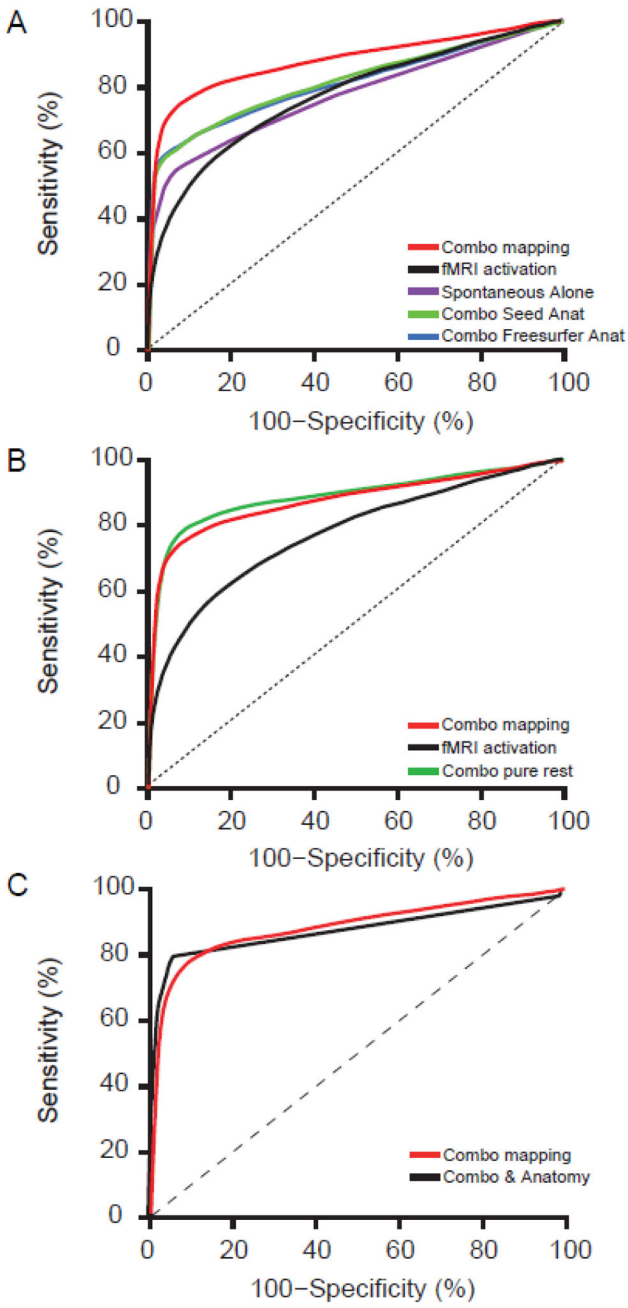

Figure 4.

Comparison of combination mapping to alternative mapping approaches using receiver operating characteristic (ROC) curves. The current combo mapping algorithm (red) outperformed traditional task activation mapping alone (black), spontaneous activity mapping alone (purple), a combination of task activation and anatomical parcellation using FreeSurfer (blue), and a combination of task activation and a priori anatomical regions of interest in the hand and tongue areas (green) (A). Combo mapping based on underlying spontaneous activity recorded during task (red) was similar to combo mapping based on "pure" spontaneous activity acquired in a dedicated resting-state scan (green) and both were

superior to traditional task activation mapping (black) (B). Adding anatomical parcellation to the current combo mapping approach (black) provided little benefit beyond standard combo mapping combining task activation and underlying spontaneous activity (red) (C).

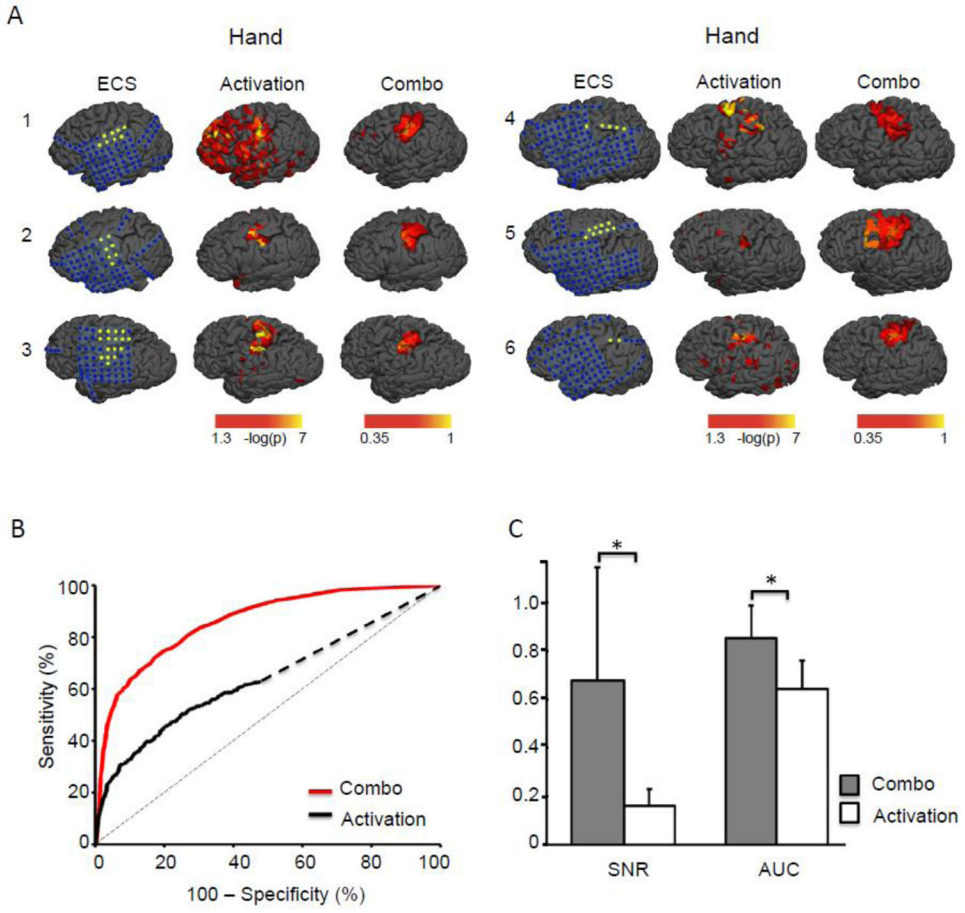

Figure 5.

Replication of combo mapping benefit in an independent dataset consisting of 6 patients. Electrical cortical stimulation (ECS), task activation, and combination mapping results are shown for each patient in DATASET 2 (A). The blue dots in the ECS maps indicate negative electrodes (no symptoms related to sensory motor cortex reported when stimulated) while the yellow dots indicate positive electrodes. Group-level receiver operating characteristic (ROC) curves (B), signal to noise ratio (C, SNR) and area under the ROC curve (C, AUC) were plotted and compared between the combo mapping approach and traditional task activation mapping. * $p < 0.01$